Synthesis and Reactivity of New Diborylphosphanes

Danan Dou,† Maomian Fan,† Eileen N. Duesler,† Heinrich Nöth,‡ and Robert T. Paine*,†

Department of Chemistry, University of New Mexico, Albuquerque, New Mexico 87131, and Institut für Anorganische Chemie, Universität München, 8000-München 2, Germany

Received December 14, 1993®

The reactions of $(i\text{-Bu}_2\text{N})_2\text{BP(H)Li·DME}$ and $(i\text{-Pr}_2\text{N})[(\text{Me}_3\text{Si})_2\text{N}]\text{BP(H)Li·DME}$ with $(\text{tmp})\text{BCl}_2$ (tmp = 2,2,6,6-tetramethylpiperidino) and $(\text{Me}_3\text{Si})_2\text{NBCl}_2$ result in the formation of diborylphosphanes $(\text{tmp})\text{B(Cl)P(H)B(N-}i\text{-Bu}_2)_2$ (**12**), $(\text{tmp})\text{B(Cl)P(H)B(N-}i\text{-Pr}_2)[\text{N(SiMe}_3)_2]$ (**14**), $(\text{Me}_3\text{Si})_2\text{NB(Cl)P(H)B(N-}i\text{-Bu}_2)_2$ (**13**), and $(\text{Me}_3\text{Si})_2\text{NB(Cl)P(H)B(N-}i\text{-Pr}_2)[\text{N(SiMe}_3)_2]$ (**15**). The diverse dehydrohalogenation chemistry of these species was studied. Combination of **12** and **13** with *t*-BuLi leads to formation of 1,3-diborylated diphosphadiboretanes, $[(i\text{-Bu}_2\text{N})_2\text{BPB(tmp)}]_2$ (**16**) and $\{(i\text{-Bu}_2\text{N})_2\text{BPB[N(SiMe}_3)_2]\}_2$ (**17**), while reaction of **14** with *t*-BuLi leads unexpectedly to a monoborylated diphosphadiboretane $[(\text{Me}_3\text{Si})_2\text{N}](i\text{-Pr}_2\text{N})\text{BPB(tmp)P(H)B(tmp)}$. Another reaction pathway is found in the reactions of **15** and $[(\text{Me}_3\text{Si})_2\text{N}]\text{B(Cl)P(H)B(N-}i\text{-Pr}_2)_2$ with *t*-BuLi that produce acyclic diphosphatriboretanes $(\text{Me}_3\text{Si})_2\text{NB}\{\text{P(H)B(N-}i\text{-Pr}_2)[\text{N(SiMe}_3)_2]\}_2$ (**19**) and $(\text{Me}_3\text{Si})_2\text{NB[P(H)B(N-}i\text{-Pr}_2)]_2$ (**20**). The molecular structures of **19**, **20**, and $[(i\text{-Pr}_2\text{N})(\text{Cl})\text{BPB(N-}i\text{-Pr}_2)]_2$ (**21**) were determined by single-crystal X-ray diffraction techniques with Mo Kα radiation (λ = 0.71073 Å): **19**, $C_{30}H_{84}B_3N_5P_2Si_6$, crystallized in the triclinic space group $P\bar{1}$ with a = 13.933(3) Å, b = 18.630(2) Å, c = 20.367(3) Å, α = 87.06(1)°, β = 80.79(1)°, γ = 88.96(2)°, and Z = 4; **20**, $C_{30}H_{76}B_3N_5P_2Si_2$, crystallized in the monoclinic space group $P2_1/c$ with a = 13.169(4) Å, b = 9.570(1) Å, c = 35.241(7) Å, β = 100.13(2)°, and Z = 4; **21** crystallized in the monoclinic space group $P2_1/n$ with a = 10.745(2) Å, b = 8.347(1) Å, c = 20.364(4) Å, β = 99.90(2)°, and Z = 4. The structural features of these compounds are discussed in relation to structures of diborylphosphanes reported previously.

Introduction

In the last few years, several new classes of boron–phosphorus compounds, including monomeric phosphinoboranes $R_2P\text{–}BR_2$, phosphanediylborates $[R'_2BPR^-]$, three-, four-, and six-membered ring P–B compounds, bicyclic and tricyclic B–P cage compounds, and metal coordination complexes of the elusive RP=BR′ double bond compounds, have been discovered.[1-3] Many of these compounds contain boron and phosphorus atoms in low-coordination environments and most are obtained by elimination of H_2, RH, LiX, HX, Me_3SiH, Me_3SiX, $P(SiMe_3)_3$, or PH_3 from appropriate coordinatively saturated phosphane borane and phosphinoborane precursors. The scope and mechanisms of these elimination reactions have attracted our interest, and some details have been elucidated. For example, we previously reported that the 1:2 combinations of several aminodichloroboranes, R_2NBCl_2 [R_2N = Me_2N, Et_2N, $i\text{-Pr}_2N$, $(Me_3Si)_2N$, Ph_2N, and tmp (2,2,6,6-tetramethylpiperidino)] with $LiPH_2$·DME result in LiCl elimination and formation of relatively unstable diphosphinoboranes, $R_2NB(PH_2)_2$. These compounds readily lose PH_3, presumably forming transient boranylidenephosphanes, $R_2NB{=}PH$, which in turn rapidly dimerize or trimerize, giving four- or six-membered ring compounds, $(R_2NBPH)_2$ [R_2N = $i\text{-Pr}_2N$, Ph_2N, tmp] and $(R_2NBPH)_3$ [R_2N = Me_2N, Et_2N, $i\text{-Pr}_2N$, $(Me_3Si)_2N$].[3]

We also reported the synthesis of a family of diborylphosphanes, $(i\text{-Pr}_2\text{N})_2\text{BP(H)B(Cl)(NR'}_2)$ (**1**), from reactions of $(i\text{-Pr}_2\text{N})_2\text{BP(H)Li·DME}$ with R'_2NBCl_2 [R'_2N = $i\text{-Pr}_2N$, $(Me_3Si)_2N$, and tmp].[4] These compounds appear ideally suited for 1,2-HCl-elimination chemistry from which one potential product would be P-borylated boranylidenephosphanes (**2**). Of course, like

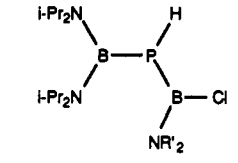

1

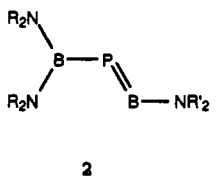

2

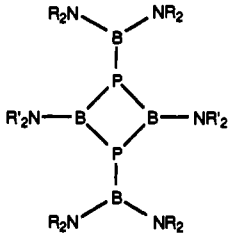

3

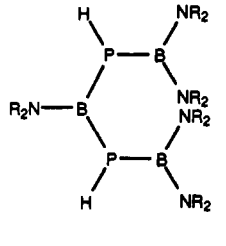

4

P-alkylated boranylidenephosphanes, RP=BR, these species may be unstable, and their subsequent reaction chemistry may be rich. We have briefly communicated the outcome of *t*-BuLi promoted dehydrohalogenation of one diborylphosphane, $(i\text{-Pr}_2\text{N})_2\text{BP(H)B(Cl)tmp}$.[5] In this case, an unusual four-membered azacarbaphosphaboretane ring formed, as summarized in Scheme 1. We report here the syntheses of additional diborylphosphanes as well as the outcome of their dehydrohalogenation chemistry. This provides the first examples of P-borylated diphosphadiboretanes (**3**) and acyclic diphosphatriboretane chains (**4**).

Experimental Section

General Information. Standard inert-atmosphere techniques were used for the manipulation of all reagents and reaction products. Infrared spectra were recorded on a Matteson 2020 FT-IR spectrometer from

† University of New Mexico.
‡ Universität München.
• Abstract published in *Advance ACS Abstracts,* April 1, 1994.

(1) Sowerby, D. B. *The Chemistry of Inorganic Homo and Heterocycles*; Haiduc, I., Sowerby, D. B., Eds.; Academic Press: New York, 1987; Vol. I, Chapter 3 and references therein.
(2) Power, P. P. *Angew. Chem., Int. Ed. Engl.* **1990**, *29*, 449 and references therein.
(3) Dou, D.; Westerhausen, M.; Wood, G. L.; Linti, G.; Duesler, E. N.; Nöth, H.; Paine, R. T. *Chem. Ber.* **1993**, *126*, 379 and references therein.
(4) Dou, D.; Wood, G. L.; Duesler, E. N.; Paine, R. T.; Nöth, H. *Inorg. Chem.* **1992**, *31*, 1695.
(5) Dou, D.; Duesler, E. N.; Paine, R. T.; Nöth, H. *J. Am. Chem. Soc.* **1992**, *114*, 9691.

0020-1669/94/1333-2151$04.50/0

Scheme 1

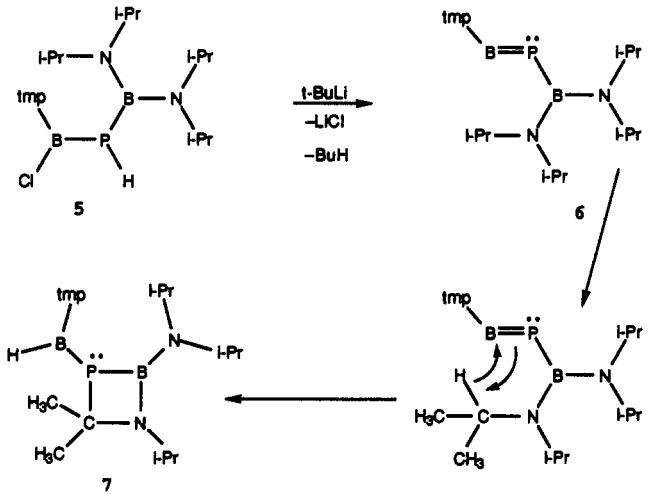

solution cells or KBr pellets. Mass spectra were obtained from a Finnegan GC/MS spectrometer by using the GC inlet system or the heated solids probe. Alternatively, mass spectra were recorded from a Kratos MS-50 spectrometer with FABS analysis or standard EI analysis. The FABS spectra and high-resolution data were recorded at the Midwest Center for Mass Spectrometry. NMR spectra were recorded on Bruker WP-250 and JEOL GSX-400 spectrometers. All NMR samples were sealed in 5-mm tubes with a deuterated lock solvent, and the spectra were referenced with Me_4Si (^{13}C, ^1H), $BF_3{\cdot}OEt_2$ (^{11}B), and 85% H_3PO_4 (^{31}P). All downfield shifts from the standard are indicated by positive δ values. Elemental analyses were obtained from the UNM analytical services laboratory.

Materials. Reagents $i\text{-}Pr_2NBCl_2$,[6] $(tmp)BCl_2$,[7] $(Me_3Si)_2NBCl_2$,[8] $(i\text{-}Pr_2N)_2BCl$,[6] $(i\text{-}Bu_2N)_2BCl$,[9] $(i\text{-}Pr_2N)[(Me_3Si)_2N]BCl$,[8] $LiPH_2{\cdot}DME$ (DME = ethylene glycol dimethyl ether),[10] and $(CO)_5Cr{\cdot}NMe_3$[11] were prepared as described in the literature. The *n*-BuLi and *t*-BuLi solutions (Aldrich) and $Fe_2(CO)_9$ (Strem) were purchased and used as received. Solvents were dried and degassed by standard methods, and solvent transfers were accomplished by vacuum distillation. All reaction and product workups were performed under dry nitrogen.

Synthesis and Characterization of Compounds. Bis(diisobutylamino)-phosphinoborane (8). A solution of $(i\text{-}Bu_2N)_2BCl$ (7.2 g, 24 mmol) in hexane (50 mL) was combined with $LiPH_2{\cdot}DME$ (3.1 g, 24 mmol) at 0 °C. The mixture was stirred at 0 °C (2 h), warmed to 23 °C, and stirred (16 h). The white, cloudy solution was filtered and the solvent removed by vacuum evaporation. Distillation [65–75 °C (10^{-3} Torr)] provided a colorless liquid: yield 6.3 g (88%). Mass spectrum (30 eV) [*m*/*z* (%)]: 299 (5, M^+), 267 (100), 259 (15), 138 (18). Infrared spectrum (neat, cm^{-1}): 2328 (w, PH), 2303 (w, PH), 1466 (vs), 1422 (vs), 1385 (s), 1366 (m), 1352 (m), 1292 (w), 1250 (s), 1223 (s), 1188 (s), 1169 (s), 1138 (s), 1099 (s), 1074 (w), 972 (w), 955 (w), 935 (w), 918 (w), 895 (w), 870 (w). Anal. Calcd for $C_{16}H_{38}BN_2P$ (M_r 300.28): C, 64.09; H, 12.76; N, 9.25. Found: C, 64.09; H, 12.45; N, 9.50.

(Bis(trimethylsilyl)amino)(diisopropylamino)phosphinoborane (9). A sample of $i\text{-}Pr_2NB(Cl)[N(SiMe_3)_2]$ (13 g, 42 mmol) in DME (50 mL) was cooled (–78 °C), and $LiPH_2{\cdot}DME$ (5.4 g, 42 mmol) was added. The mixture was held at –78 °C (2 h), warmed, and stirred at 23 °C (16 h). The solvent was removed by vacuum evaporation, and hexane (25 mL) was added to the residue. The resulting solution was filtered and the solvent removed by vacuum evaporation. The crude product was vacuum distilled [60–70 °C (10^{-3} Torr)], and a clear, colorless liquid was collected: yield 10.8 g, (85%). Mass spectrum (30 eV) [*m*/*z* (%)]: 289 (1, M^+ – Me), 271 (98), 229 (100), 172 (50), 98 (60). Infrared spectrum (hexane, cm^{-1}): 2338 (w, PH), 2324 (w, PH), 1437 (w), 1368 (w), 1319 (w), 1302 (m), 1252 (m), 1186 (w), 1086 (w), 1053 (m), 924 (s), 883 (m), 839 (m), 679 (w). Anal. Calcd for $C_{12}H_{34}BN_2Si_2P$ (M_r 304.38): C, 47.35; H, 11.26; N, 9.20. Found: C, 47.85; H, 11.74; N, 9.12.

Lithium–Dimethoxyethane [Bis(diisobutylamino)boryl]phosphide (10). A solution of **8** (11 g, 37 mmol) in DME (50 mL) was cooled (–78 °C), and *n*-BuLi (15 mL, 2.5 M solution in hexane, 37 mmol) was added dropwise with stirring. The mixture was stirred at –78 °C (2 h) and then at 23 °C (16 h). The yellow solution was filtered and the solvent removed by vacuum evaporation. The solid residue was recrystallized twice (–10 °C) from hexane, leaving a white solid: yield 10.8 g (74%); mp 97–99 °C. Infrared spectrum (hexane, cm^{-1}): 2280 (w, PH), 1445 (w), 1420 (m), 1389 (s), 1366 (m), 1329 (m), 1294 (w), 1271 (w), 1234 (s), 1194 (s), 1115 (vs), 1092 (vs), 1032 (w), 1018 (w), 970 (w), 934 (w), 918 (w), 870 (w). Anal. Calcd for $C_{20}H_{47}LiBN_2O_2P$ (M_r 396.33): C, 60.61; H, 11.95; N, 7.07. Found: C, 60.86; H, 12.31; N, 7.50.

Lithium–Dimethoxyethane [(Bis(trimethylsilyl)amino)(diisopropylamino)boryl]phosphide (11). A solution of **9** (0.5 g, 1.6 mmol) in DME (25 mL) was cooled (–78 °C), and *t*-BuLi (1 mL of 1.7 M solution) was added dropwise from a syringe. The yellow solution was stirred at –78 °C (2 h), warmed to 23 °C, and stirred (12 h). The solvent was removed by vacuum evaporation, and the yellow residue was recrystallized from hexane (–10 °C), leaving colorless crystals: yield 0.4 g (63%); mp 184–186 °C. Infrared spectrum (hexane, cm^{-1}): 2276 (w, PH), 1437 (w), 1416 (w), 1364 (w), 1317 (w), 1302 (w), 1258 (s), 1209 (w), 1188 (m), 1142 (m), 1128 (m), 1113 (m), 1090 (m), 1047 (s), 1003 (w), 945 (s), 926 (m), 887 (s), 837 (s), 667 (w). Anal. Calcd for $C_{15.36}H_{41.4}LiBN_2O_{1.68}Si_2P$ (M_r 386.01):[12] C, 47.79; H, 10.81; N, 7.26. Found: C, 47.52; H, 11.01; N, 7.18.

[Bis(diisobutylamino)boryl][(2,2,6,6-tetramethylpiperidino)chloroboryl]-phosphane (12). A solution of $(tmp)BCl_2$ (4.3 g, 19 mmol) in hexane (50 mL) was combined with **10** (7.7 g, 19 mmol) at –78 °C and stirred (16 h). The yellow, cloudy solution was filtered and the solvent removed by vacuum evaporation, leaving a yellow oil that could not be distilled without decomposition: yield 9.4 g (99%). Mass spectrum (30 eV) [*m*/*z* (%)]: 485 (1, M^+), 267 (100), 138 (10). Infrared spectrum (hexane, cm^{-1}): 2349 (w, PH), 1464 (s), 1422 (s), 1387 (s), 1366 (s), 1323 (s), 1283 (m), 1250 (s), 1219 (m), 1186 (s), 1169 (s), 1134 (s), 1096 (s), 995 (m), 972 (m), 937 (w), 918 (w), 883 (w), 856 (m), 842 (m), 787 (m), 665 (w), 569 (w), 519 (w). Anal. Calcd for $C_{25}H_{55}B_2N_3PCl$ (M_r 484.78): C, 61.81; H, 11.41; N, 8.65. Found: C, 62.81; H, 12.35; N, 8.64.

[Bis(diisobutylamino)boryl]{[bis(trimethylsilyl)amino]chloroboryl}-phosphane (13). A solution of $(tms)_2NBCl_2$ (3.3 g, 13 mmol) in hexane (25 mL) was combined with **10** (5.4, 13 mmol) at 23 °C. The mixture was stirred at 23 °C (16 h) and filtered, and the filtrate was vacuum evaporated. The residue was recrystallized in hexane (–10 °C), and a white solid was obtained: yield 4.4 g (64%); mp 94–96 °C. Mass spectrum (30 eV) [*m*/*z* (%)]: 505 (1, M^+), 267 (100), 138 (10). Infrared spectrum (hexane, cm^{-1}): 2340 (w, PH), 1479 (w), 1422 (vs), 1387 (m), 1368 (m), 1335 (m), 1302 (m), 1254 (vs), 1233 (s), 1219 (s), 1184 (s), 1167 (s), 1138 (s), 1094 (vs), 972 (w), 955 (w), 914 (s), 851 (vs), 791 (w), 765 (w), 681 (w), 667 (w), 621 (w). Anal. Calcd for $C_{22}H_{55}B_2N_3Si_2PCl$ (M_r 505.92): C, 52.23; H, 10.96; N, 8.30. Found: C, 52.18; H, 11.44; N, 8.46.

[(Bis(trimethylsilyl)amino)(diisopropylamino)boryl][2,2,6,6-tetramethylpiperidino)chloroboryl]phosphane (14). A solution of $(tmp)BCl_2$ (2.2 g, 9.9 mmol) in hexane (25 mL) was combined with **11** (4.0 g, 9.9 mmol) in hexane (25 mL) at 23 °C. The solution was stirred (2 d) and then filtered. The filtrate was concentrated, and colorless crystals deposited from the solution (–10 °C): yield 3.2 g (66%); mp 97–99 °C. Mass spectrum (30 eV) [*m*/*z* (%)]: 271 (100), 229 (38). Infrared spectrum (hexane, cm^{-1}): 2353 (w, PH), 1420 (s), 1387 (s), 1368 (vs), 1346 (s), 1319 (vs), 1285 (s), 1252 (vs), 1194 (s), 1171 (s), 1155 (s), 1128 (s), 1070 (vs), 993 (s), 972 (s), 918 (vs), 887 (vs), 841 (vs), 787 (m), 770 (m), 758 (m), 677 (m), 519 (w). Anal. Calcd for $C_{21}H_{51}B_2N_3Si_2PCl$ (M_r 489.89): C, 51.49; H, 10.49; N, 8.58. Found: C, 51.38; H, 10.71; N, 8.42.

{[Bis(trimethylsilyl)amino][(diisopropylamino)boryl]{[bis(trimethylsilyl)-amino]chloroboryl}phosphane (15). A solution of $(tms)_2NBCl_2$ (0.7 g, 2.9 mmol) in hexane (50 mL) was combined with **11** (1.1 g, 2.9 mmol) at 23 °C, and the mixture was stirred (2 d). The white, cloudy solution was filtered, the solvent removed from the filtrate by vacuum evaporation, and the solid residue was recrystallized in hexane (–10 °C), leaving

(6) Gerrard, W.; Hudson, H. R.; Mooney, E. R. *J. Chem. Soc.* **1960**, 5168.
(7) Nöth, H.; Weber, S. *Z. Naturforsch, B* **1983**, *37*, 1460.
(8) $(Me_3Si)_2NBCl_2$ was prepared by a modification of the literature method: Geymayer, P.; Rochow, E. G. *Monatsh. Chem.* **1966**, *97*, 429.
(9) $(i\text{-}Bu_2N)_2BCl$ was prepared by a modification of the method used to prepare $(i\text{-}Pr_2N)_2BCl$.[6]
(10) Schäfer, H.; Fritz, G.; Holderich, W. *Z. Anorg. Allg. Chem.* **1977**, *428*, 222.
(11) Wasserman, H. J.; Workulich, M.; Atwood, J. D.; Churchill, M. R. *Inorg. Chem.* **1980**, *19*, 2831.

(12) This composition corresponds to a solvate of **12** with 0.84 equivalent of DME per equivalent of salt.

Table 1. Crystallographic Data for $(Me_3Si)_2NB\{P(H)B(N\text{-}i\text{-}Pr_2)[N(SiMe_3)_2]\}_2$ (**19**), $(Me_3Si)_2NB[P(H)B(N\text{-}i\text{-}Pr_2)_2]_2$ (**20**), and $\{[(i\text{-}Pr_2N)(Cl)B]PB(N\text{-}i\text{-}Pr_2)\}_2$ (**21**)

	19	**20**	**21**
chem formula	$C_{30}H_{84}B_3N_5P_2Si_6$	$C_{30}H_{76}B_3N_5P_2Si_2$	$C_{12}H_{28}B_2N_2PCl$
a, Å	13.933(3)	13.169(4)	10.745(2)
b, Å	18.630(2)	9.570(1)	8.347(1)
c, Å	20.367(3)	35.241(7)	20.364(4)
α, deg	87.06(1)	90	90
β, deg	80.79(1)	100.13(2)	99.90(2)
γ, deg	88.96(2)	90	90
V, Å^3	5211.4(2)	4372(2)	1799.2(7)
Z	4	4	4
ρ_{calcd}, g cm^{-3}	0.991	0.999	1.065
fw	777.9	657.5	288.4
cryst dimens, mm	0.21 × 0.28 × 0.51	0.16 × 0.25 × 0.60	0.09 × 0.12 × 0.51
cryst syst	triclinic	monoclinic	monoclinic
space group	$P\bar{1}$	$P2_1/c$	$P2_1/n$
T, °C	20	20	20
μ, mm^{-1}	0.240	0.174	0.286
2θ range, deg	2–45	2–45	2–40
reflcns measd	$\pm h,-k,\pm l$	$+h,+k,\pm l$	$\pm h,\pm k,\pm l$
total no. of reflcns collcd	14168	6454	6670
no. of unique reflcns	13657	5713	1670
no. of obsd reflcns	7571 ($F > 2\sigma(F)$)	3123 ($F > 2\sigma(F)$)	1321 ($F > 2\sigma(F)$)
transm coeff: min/max	0.824/0.852	0.785/0.819	0.826/0.842
R_F	9.13	9.86	11.24
R_{wF}	6.55	7.06	5.89

colorless crystals: yield 1.0 g (68%); mp 85–87 °C. Mass spectrum (30 eV) [m/z (%)]: 271 (100), 229 (22), 172 (8), 98 (15). Infrared spectrum (hexane, cm^{-1}): 2342 (w, PH), 1424 (m), 1366 (m), 1327 (s), 1298 (s), 1254 (s), 1221 (s), 1194 (s), 1138 (s), 1121 (s), 1070 (s), 914 (vs), 873 (vs), 851 (vs), 768 (m), 679 (m), 626 (w). Anal. Calcd for $C_{18}H_{51}B_2N_3Si_4PCl$ (510.03): C, 42.39; H, 10.08; N, 8.24. Found: C, 42.39; H, 10.15; N, 7.95.

2,4-Bis(2,2,6,6-tetramethylpiperidino)-1,3-[bis(diisobutylamino)boryl]-1,3,2,4-diphosphadiboretane (16). A solution of **12** (8.8 g, 18 mmol) in hexane (50 mL) was cooled (–78 °C), and t-BuLi (10.7 mL, 1.7 M solution) in pentane was added dropwise. The reaction mixture was stirred (2 h, –78 °C) and then warmed and stirred (23 °C, 16 h). The yellow, cloudy solution was filtered and the solvent removed by vacuum evaporation. Yellow crystals deposited from the oily residue upon standing at 23 °C overnight: yield 5.0 g (61%); mp 167–169 °C. Mass spectrum; (HRFAB) 897.8654 (M^+, $C_{50}H_{108}{}^{11}B_3{}^{10}BN_6P_2$, 897.8633); (EI, 30 eV) [m/z (%)] 503 (10), 450 (32), 267 (100), 223 (8), 139 (10). Infrared spectrum (hexane, cm^{-1}): 1478 (w), 1404 (s), 1364 (s), 1333 (s), 1304 (s), 1273 (s), 1244 (s), 1209 (s), 1171 (s), 1130 (s), 1088 (s), 1042 (w), 1005 (m), 974 (m), 941 (w), 910 (m), 866 (m), 828 (w), 754 (w), 702 (w), 561 (w). Anal. Calcd for $C_{50}H_{108}B_4N_6P_2$ (M_r 898.64): C, 66.83; H, 12.11; N, 9.35. Found: C, 66.79; H, 13.20; N, 9.60.

2,4-Bis(bis(trimethylsilyl)amino)-1,3-[bis(diisobutylamino)boryl]-1,3,2,4-diphosphadiboretane (17). A solution of **13** (2.9 g, 5.7 mmol) in hexane (50 mL) was cooled (–78 °C), and t-BuLi (3.4 mL, 1.7 M solution in pentane) was added dropwise. The reaction mixture was briefly stirred (–78 °C), and then warmed and stirred (50 °C, 2 d). The yellow, cloudy solution was filtered and the solvent removed by vacuum evaporation, leaving a yellow oil. Yellow crystals deposited from the oily residue upon standing: yield 0.6 g (22%); mp 160–162 °C. Mass spectrum: (HRFAB) 939.7615 (M^+, $C_{44}H_{109}{}^{11}B_4N_6{}^{28}Si_4P_2$ 939.7638); (EI, 30 eV) [m/z (%)] 299 (100), 267 (58), 172 (17). Infrared spectrum (hexane, cm^{-1}): 1412 (s), 1387 (m), 1368 (w), 1335 (w), 1250 (s), 1211 (m), 1165 (vs), 1086 (s), 966 (w), 955 (w), 910 (s), 862 (vs), 764 (w), 679 (w), 623 (w). Anal. Calcd for $C_{44}H_{108}B_4N_6Si_4P$ (M_r 938.92): C, 56.29; H, 11.59; N, 8.95. Found: C, 56.53; H, 11.86; N, 8.92.

2-[(Bis(trimethylsilyl)amino)(diisopropylamino)boryl]-1,3-bis(2,2,6,6-tetramethylpiperidino)-1,3,2,4-diphosphadiboretane (18). A sample of tmpB[P(H)B(tmp)]PLi·DME (1.9 g, 4.2 mmol) was suspended in hexane (30 mL) and $(i\text{-}Pr_2N)[(Me_3Si)_2N]BCl$ (1.3 g, 4.2 mmol) in hexane (20 mL) was added with stirring (–78 °C). The mixture was warmed slowly (2 h) to 23 °C and stirred (16 h). The resulting cloudy mixture was filtered, and the filtrate was evaporated, leaving a pale yellow, oily solid. Recrystallization from hexane (–10 °C) provided a colorless crystalline solid: yield 2.1 g (78%); mp 172–174 °C. Mass spectrum (30 eV) [m/e (%)] 637 (0.2, M^+), 621 (2), 400 (2), 364 (7), 349 (2), 271 (100), 229 (20). Infrared spectrum (hexane, cm^{-1}): 2204 (w), 1361 (m), 1315 (s), 1298 (s), 1284 (s), 1190 (m), 1168 (m), 1130 (w), 1111 (w), 1037 (m), 987 (w), 908 (m), 881 (s), 837 (s). Anal. Calcd for $C_{30}H_{69}B_3N_4P_2Si_2$ (M_r 636.47): C, 56.61; H, 10.93; N, 8.80. Found: C, 57.00; H, 11.03; N, 8.77.

Bis{bis[((bis(trimethylsilyl)amino)(diisopropylamino)boryl]phosphino}-bis(trimethylsilylamino)borane (19). A sample of t-BuLi (3.8 mL of 1.7 M solution in pentane) was added to **15** (3.3 g, 6.5 mmol) in 20 mL of pentane (–78 °C). The mixture was stirred (2 h), warmed, stirred at 23 °C (2 h), and then heated at 50 °C (16 h). The yellow, cloudy solution was filtered, and the majority of the solvent was removed from the filtrate. Yellow crystals deposited from the concentrated (~5 mL) solution upon cooling (–10 °C): yield 1.6 g (32%); mp 142–144 °C. Mass spectrum (30 eV) [m/z (%)]: 271 (100). Infrared spectrum (hexane, cm^{-1}): 2351 (w, PH), 1418 (w), 1364 (w), 1323 (m), 1250 (s), 1196 (m), 1134 (m), 1121 (m), 1057 (s), 916 (s), 880 (s), 841 (vs), 795 (w), 758 (w), 741 (w), 679 (w). Anal. Calcd for $C_{30}H_{84}B_3N_5Si_6P_2$ (M_r 777.92): C, 46.32; H, 10.88; N, 9.00. Found: C, 46.31; H, 11.51; N, 9.10.

Bis{[bis(diisopropylamino)boryl]phosphino}bis(trimethylsilylamino)-borane (20). A sample of t-BuLi (11.8 mL, 1.7 M solution in pentane) was added to a cooled (–78 °C) hexane solution of $(Me_3Si)_2NB(Cl)P(H)B(N\text{-}i\text{-}Pr_2)_2$[3] (9.0 g, 20 mmol). The mixture was stirred (2 h) and then warmed and stirred at 23 °C (24 h). The yellow, cloudy solution was filtered and the solvent removed from the filtrate by vacuum evaporation. Colorless crystals were isolated after recrystallization in hexane (–10 °C): yield 1.5 g (11%); mp 120–122 °C. Mass spectrum (30 eV) [m/z (%)]: 609 (1), 513 (1), 436 (1), 414 (5), 406 (3), 373 (5), 241 (2), 211 (100). Infrared spectrum (hexane, cm^{-1}): 2311 (w, PH), 1412 (s), 1362 (s), 1308 (s), 1250 (s), 1221 (s), 1198 (vs), 1130 (vs), 1074 (w), 995 (w), 932 (m), 907 (s), 872 (vs), 845 (vs), 797 (m), 762 (m), 679 (w), 650 (w). Anal. Calcd for $C_{30}H_{76}B_3N_5Si_2P_2$ (M_r 657.52): C, 54.80; H, 11.56; N, 10.65. Found: C, 55.20; H, 12.45; N, 10.84.

2,4-Bis[(diisopropylamino)chloroboryl]-1,3-bis(diisopropylamino)-1,3,2,4-diphosphadiboretane (21). Method a. A sample of $i\text{-}Pr_2NBCl_2$ (0.80 g, 4.4 mmol) was diluted in hexane (50 mL) and added at –78 °C to $i\text{-}Pr_2N$B[P(H)B(N-i-Pr$_2$)]PLi·DME$_3$ (1.7 g, 4.4 mmol) in hexane (20 mL). The mixture was stirred (2 h) and then warmed and stirred at 23 °C (16 h). The cloudy, yellow mixture was filtered and concentrated to ~5 mL, and colorless crystals deposited upon standing overnight (23 °C): yield 0.2 g (8%); mp 202–204 °C. Mass spectrum (30 eV) [m/z (%)]: 430 (30), 395 (12), 253 (100), 167 (55), 110 (35). Infrared spectrum (hexane, cm^{-1}): 1474 (w), 1439 (m), 1368 (m), 1304 (s), 1186 (m), 1140 (s), 1003 (m), 867 (w), 810 (w), 577 (w). Anal. Calcd for $C_{24}H_{56}B_4N_4P_2Cl_2$ (M_r 576.83): C, 49.97; H, 9.78; N, 9.71. Found: C, 50.13; H, 9.88; N, 9.77.

Method b. A sample of $(MeN)_3(MeB)_2BP(H)Li\cdot DME$[13] (2.6 g, 9.3 mmol) in DME (20 mL) was added (–78 °C) to $i\text{-}Pr_2NBCl_2$ (1.7 g, 9.3 mmol) in hexane (30 mL). The mixture was stirred (2 h) and then warmed and stirred at 23 °C (16 h). The slurry was filtered, the solvent vacuum evaporated from the filtrate, and 2.8 g of crude product obtained. This material was redissolved in hexane (~20 mL) and cooled (–10 °C). Colorless needles (1.0 g, 5.0 mmol) identified as $(MeN)_3(MeB)_2BCl$ were deposited. The remaining supernatant solution was decanted, concentrated to ~8 mL, and cooled (–10 °C). Colorless crystals of **21** (0.4 g, 0.7 mmol) formed and were recrystallized from hexane (5 mL): yield 30%; mp 204–206 °C. Mass spectrum (30 eV) [m/z (%)]: 577 (M^+, 100), 534 (5), 430 (30), 395 (17), 253 (100), 167 (40), 146 (25), 110 (23). Anal. Found: C, 50.11; H, 10.97; N, 9.84.

Coordination Complexes. $(CO)_5Cr(21)$. A sample of **21** (0.43 g, 0.75 mmol) and $(CO)_5Cr{\cdot}NMe_3$ (0.19 g, 0.75 mmol) were combined in hexane (25 mL). The mixture was stirred (16 h), and then the solvent was removed by vacuum evaporation and the residue recrystallized from hexane (–10 °C). Yellow crystals deposited and were collected by decanting the mother liquor: yield 0.4 g (70%); mp: 179–181 °C. Mass spectrum: (HRFAB) 768.2890 (M^+, $C_{29}H_{56}{}^{11}B_4N_4O_5P_2{}^{35}Cl_2{}^{52}Cr$, 768.288036); (EI, 30 eV) 768 (M^+, 1), 628 (40), 576 (12), 430 (8), 395 (12), 253 (46), 154 (54), 138 (52), 102 (100). Infrared spectrum (hexane, cm^{-1}): 2054

(13) Fan, M.; Dou, D.; Duesler, E. N.; Paine, R. T. To be submitted for publication.

Table 2. Atomic Coordinates (×10⁴) and Their Esd's for $(Me_3Si)_2NB\{P(H)B(N\text{-}i\text{-}Pr_2)[N(SiMe_3)_2]\}_2$ (**19**)

	x	y	z		x	y	z
P(1)	1279(1)	3899(1)	1507(1)	P(3)	4646(1)	1085(1)	8462(1)
P(2)	2322(1)	3820(1)	2845(1)	P(4)	6359(1)	1187(1)	7151(1)
Si(1)	3688(2)	4203(1)	831(1)	Si(7)	7039(2)	2299(1)	8550(1)
Si(2)	3766(2)	2685(1)	1497(1)	Si(8)	6779(1)	753(1)	9153(1)
Si(3)	-883(2)	2573(1)	2107(2)	Si(9)	2772(2)	2423(1)	7810(1)
Si(4)	-1140(2)	3671(2)	972(1)	Si(10)	1912(2)	1331(2)	8898(1)
Si(5)	2589(2)	2444(1)	4265(1)	Si(11)	7270(2)	2586(1)	5747(1)
Si(6)	2184(2)	3947(1)	4770(1)	Si(12)	7149(2)	1090(1)	5229(1)
B(1)	2406(6)	3710(4)	1928(4)	B(4)	5975(6)	1283(4)	8068(4)
B(2)	-57(6)	3916(5)	1943(4)	B(5)	3552(6)	1064(4)	7976(4)
B(3)	3167(6)	3698(4)	3504(4)	B(6)	7514(6)	1317(4)	6490(4)
N(1)	3295(3)	3565(3)	1471(2)	N(6)	6631(3)	1417(3)	8540(2)
N(2)	-722(3)	3417(3)	1709(3)	N(7)	2738(4)	1572(3)	8189(2)
N(3)	-375(3)	4459(3)	2390(3)	N(8)	3489(3)	520(3)	7540(3)
N(4)	2696(4)	3375(3)	4155(3)	N(9)	7357(4)	1656(3)	5845(3)
N(5)	4110(4)	3978(3)	3395(2)	N(10)	8419(4)	1040(3)	6607(3)
C(1)	3223(5)	4067(5)	45(3)	C(31)	8286(5)	2407(4)	8098(4)
C(2)	5045(5)	4160(4)	653(4)	C(32)	6218(6)	2934(4)	8179(5)
C(3)	3330(5)	5113(4)	1113(3)	C(33)	7020(6)	2574(5)	9412(4)
C(4)	4811(5)	2622(4)	1959(4)	C(34)	5937(5)	839(4)	9949(3)
C(5)	2799(6)	2051(4)	1885(5)	C(35)	6608(5)	-142(3)	8835(3)
C(6)	4186(6)	2397(5)	633(4)	C(36)	8041(5)	796(4)	9340(3)
C(7)	-107(6)	2442(4)	2736(5)	C(37)	1717(5)	2603(4)	7368(4)
C(8)	-2174(6)	2442(5)	2526(5)	C(38)	3870(5)	2526(4)	7180(4)
C(9)	-560(8)	1845(6)	1507(6)	C(39)	2808(8)	3120(4)	8419(5)
C(10)	-396(7)	3312(7)	238(4)	C(40)	1674(8)	338(5)	8953(5)
C(11)	-2405(6)	3394(8)	998(5)	C(41)	726(5)	1770(6)	8900(4)
C(12)	-1099(9)	4668(6)	819(6)	C(42)	2350(6)	1515(7)	9675(4)
C(13)	1390(7)	2116(5)	4152(5)	C(43)	6007(7)	2921(5)	5838(5)
C(14)	3504(7)	1987(4)	3682(5)	C(44)	7887(7)	2901(4)	4918(4)
C(15)	2771(7)	2140(4)	5115(4)	C(45)	7851(8)	3031(4)	6376(4)
C(16)	2219(6)	4889(4)	4455(4)	C(46)	7102(6)	147(4)	5526(4)
C(17)	2836(8)	3914(5)	5510(4)	C(47)	6006(8)	1322(6)	4940(6)
C(18)	907(7)	3720(5)	5065(5)	C(48)	8145(8)	1151(5)	4481(4)
C(19)	318(5)	5021(4)	2506(5)	C(49)	2635(5)	468(4)	7194(4)
C(20)	302(6)	5677(5)	2017(6)	C(50)	2161(5)	-265(4)	7254(4)
C(21)	260(6)	5237(5)	3214(5)	C(51)	2810(6)	759(4)	6480(4)
C(22)	-1408(5)	4493(4)	2720(4)	C(52)	4263(5)	-43(4)	7449(4)
C(23)	-1904(5)	5215(4)	2638(4)	C(53)	4023(6)	-696(4)	7944(5)
C(24)	-1580(6)	4215(5)	3436(4)	C(54)	4603(6)	-261(5)	6754(5)
C(25)	4748(7)	3861(5)	3913(4)	C(55)	9298(6)	1165(5)	6094(4)
C(26)	5571(6)	3317(6)	3733(5)	C(56)	9826(6)	486(5)	5830(4)
C(27)	5103(7)	4546(5)	4166(4)	C(57)	10006(6)	1695(5)	6295(4)
C(28)	4441(5)	4437(4)	2788(3)	C(58)	8492(5)	560(4)	7206(4)
C(29)	4155(6)	5218(4)	2880(4)	C(59)	8307(6)	-221(4)	7103(4)
C(30)	5511(5)	4374(5)	2488(4)	C(60)	9400(5)	630(5)	7527(4)

(m), 1971 (w), 1956 (w), 1929 (vs), 1479 (w), 1441 (w), 1369 (w), 1309 (m), 1184 (w), 1142 (w), 1115 (w), 1001 (w), 879 (w), 673 (m), 655 (m), 463 (w). Anal. Calcd for $C_{29}H_{56}B_4N_4O_5P_2Cl_2Cr$ (M_r 768.68): C, 45.31; H, 7.34; N, 7.29. Found: C, 45.14; H, 7.26; N, 7.27.

$(CO)_3Fe$(21). A sample of $Fe_2(CO)_9$ (0.13 g, 0.35 mmol) was combined with **21** (0.2 g, 0.35 mmol) in hexane (25 mL). The mixture was stirred at 23 °C (16 h), the solution was filtered, and the solvent was removed by vacuum evaporation. The residue was recrystallized from hexane (-10 °C), leaving a gold-brown solid: yield 0.2 g (80%); mp 172–174 dec. Mass spectrum: (HRFAB) 716.2928 (M^+, $C_{27}H_{56}{}^{11}B_4N_4O_3P_2{}^{35}Cl_2{}^{56}Fe$, 716.292623); (EI, 30 eV) 716 (1), 632 (10), 253 (18), 136 (19), 102 (100). Infrared spectrum (hexane, cm^{-1}): 2035 (s), 1958 (s), 1931 (s), 1919 (vs), 1476 (w), 1458 (w), 1443 (w), 1381 (w), 1369 (w), 1312 (m), 1184 (w), 1142 (w), 1117 (w), 1001 (w), 880 (w), 822 (w), 725 (w), 623 (w). Anal. Calcd for $C_{27}H_{56}B_4N_4O_3P_2Cl_2Fe$ (M_r 716.71): C, 45.25; H, 7.88; N, 7.82. Found: C, 45.06; H, 8.04; N, 7.58.

Crystallographic Measurements and Structure Solutions. Crystals of **19**, **20**, and **21** were placed in glass capillaries under dry nitrogen. The crystals were centered on a Siemens R3m/V automated diffractometer, and determinations of the crystal classes, orientation matrices, and unit cell dimensions were performed in a standard manner. Data were collected in θ–2θ (**20**) and ω (**19**,**21**) scan modes with Mo Kα (λ = 0.710 73 Å) radiation, a scintillation counter, and pulse height analyzer. Selected data collection parameters are summarized in Table 1. In each case, inspection of a small data set led to assignment of the space groups.[14] Small, semiempirical absorption corrections were applied based on ψ scans.[15]

All calculations were performed on a Siemens SHELXTL PLUS (VMS version) structure determination system.[16] Structure solutions were by direct methods, and full-matrix refinements were employed.[17] Neutral atom scattering factors and anomalous dispersion terms were used for all non-hydrogen atoms during the refinements. The function minimized was $\sum w(|F_o| - |F_c|)^2$. For **19** and **20**, there was a slow, steady decay of the standard reflections during data collection. The average losses in intensity were ~7% and ~10%, respectively. The data were scaled accordingly. There are two independent, but chemically equivalent, molecules of **19** in the asymmetric unit. Hydrogen atoms on carbon

(14) Space group notation is given in *International Tables for X-Ray Crystallography*; Reidel: Dordrecht, The Netherlands, 1983; Vol. I, pp 73–346.

(15) The empirical absorption corrections use an ellipsoidal model fitted to azimuthal scan data that are then applied to the intensity data: *SHELXTL Manual, Revision 4*; Nicolet XRD Corp.: Madison, WI, 1983.

(16) Sheldrick, G. M. *Nicolet SHELXTL Operations Manual*: Nicolet XRD Corp.: Cupertino, CA, 1981. SHELXTL uses absorption, anomalous dispersion, and scattering data compiled in: *International Tables for X-Ray Crystallography*; Kynoch: Birmingham, England, 1974; Vol. IV, pp 55–60, 99–101, 149–150. Anomalous dispersion terms were included for all atoms with atomic numbers greater than 2.

(17) A general description of the least-squares algebra is found in: *Crystallographic Computing*; Ahmed, F. R., Hall, S. R., Huber, C. P., Eds.; Munksgaard: Copenhagen, 1970; p 187. The least-squares refinement minimizes $\sum w(|F_o| - F_c|)^2$, where $w = 1/[\sum(F)^2 + gF^2]$. $R = \sum||F_o| - |F_c||/\sum|F_o|$, $R_{wF} = [[\sum(|F_o| - |F_c|)^2/\sum wF_o^2]$, and GOF = $[[\sum w(|F_o| - F_c|)^2/(NO - NV)]$, where NO = number of observations and NV = number of variables.

Table 3. Atomic Coordinates (×10⁴) and Their Esd's for $(Me_3Si)_2NB[P(H)B(N\text{-}i\text{-}Pr_2)_2]_2$ (**20**)

	x	y	z
P(1)	2096(2)	7587(2)	3712(1)
P(2)	255(2)	6307(3)	4115(1)
Si(1)	3241(2)	8118(3)	4656(1)
C(1)	4383(6)	7968(9)	4417(2)
C(2)	2599(7)	9827(9)	4549(3)
C(3)	3761(7)	8197(10)	5185(2)
Si(2)	2223(2)	5400(3)	4868(1)
C(4)	3512(6)	4737(9)	5101(2)
C(5)	1497(7)	6052(10)	5242(2)
C(6)	1562(6)	3812(8)	4645(2)
B(1)	1682(7)	6809(9)	4165(3)
B(2)	2995(8)	6627(11)	3409(3)
B(3)	−712(7)	7415(12)	3741(3)
N(1)	2371(4)	6725(6)	4533(2)
N(2)	3069(5)	7301(7)	3048(2)
N(3)	3550(5)	5387(7)	3527(2)
N(4)	−1078(5)	8701(8)	3872(2)
N(5)	−1122(5)	6841(7)	3376(2)
C(7)	2959(8)	6436(10)	2696(2)
C(8)	3830(9)	6599(11)	2461(3)
C(9)	1915(8)	6646(11)	2433(2)
C(10)	3162(9)	8808(12)	2982(3)
C(11)	2201(9)	9677(10)	2971(3)
C(12)	4072(9)	9429(11)	3240(3)
C(13)	4569(7)	5159(10)	3403(3)
C(14)	4702(7)	3755(10)	3211(3)
C(15)	5495(7)	5499(11)	3716(3)
C(16)	3149(6)	4352(9)	3767(2)
C(17)	2563(6)	3178(9)	3525(2)
C(18)	3922(7)	3732(10)	4096(2)
C(19)	−2190(7)	8900(9)	3846(2)
C(20)	−2585(6)	8433(11)	4212(3)
C(21)	−2621(7)	10327(10)	3719(3)
C(22)	−345(7)	9712(10)	4071(3)
C(23)	−482(8)	10149(11)	4472(3)
C(24)	−92(7)	10878(10)	3825(3)
C(25)	−1582(6)	7786(9)	3057(2)
C(26)	−2715(6)	7423(10)	2888(2)
C(27)	−916(7)	7833(9)	2744(2)
C(28)	−1100(7)	5335(9)	3265(2)
C(29)	−39(6)	4751(9)	3248(2)
C(30)	−1683(6)	4414(9)	3502(3)

Table 4. Atomic Coordinates (×10⁴) and Their Esd's for $\{[(i\text{-}Pr_2N)(Cl)B]PB(N\text{-}i\text{-}Pr_2)\}_2$ (**21**)

	x	y	z
P(1)	4882(2)	−1550(3)	306(1)
B(1)	6022(8)	231(11)	394(4)
N(1)	7175(6)	587(8)	803(3)
C(1)	7777(9)	−434(12)	1366(5)
C(2)	7029(8)	−419(11)	1931(4)
C(4)	7952(8)	1991(10)	677(4)
C(5)	9127(7)	1473(10)	412(4)
C(6)	8213(7)	3183(9)	1237(4)
B(2)	3890(8)	−1666(12)	1025(4)
Cl	3459(3)	168(3)	1353(1)
N(2)	3541(5)	−3120(7)	1264(3)
C(7)	2828(7)	−3320(10)	1831(4)
C(8)	3576(7)	−2681(9)	2491(3)
C(9)	1499(7)	−2655(10)	1700(3)
C(10)	3853(8)	−4686(9)	997(4)
C(11)	2673(7)	−5634(8)	698(4)
C(12)	4762(7)	−5645(8)	1482(4)

atoms of **19** and **20** were included in idealized positions (riding model) with $U_{iso} = 1.25U_{eq}$ of the parent atom. Difference maps gave the positions of the hydrogen atoms on the phosphorus atoms, and there were refined in fixed positions.

The final non-hydrogen atom positional parameters are listed in Tables 2–4, and selected bond distances and angles are summarized in Table 5.

Results and Discussion

As described previously for other diaminochloroboranes,[4] the reactions of $(i\text{-}Bu_2N)_2BCl$ and $(i\text{-}Pr_2N)[(Me_3Si)_2N]BCl$ with $LiPH_2\cdot DME$ produce high yields of diaminophosphinoboranes, $(i\text{-}Bu_2N)_2BPH_2$ (**8**) and $(i\text{-}Pr_2N)[(Me_3Si)_2N]BPH_2$ (**9**), as summarized in eq 1. Both compounds are characterized by two

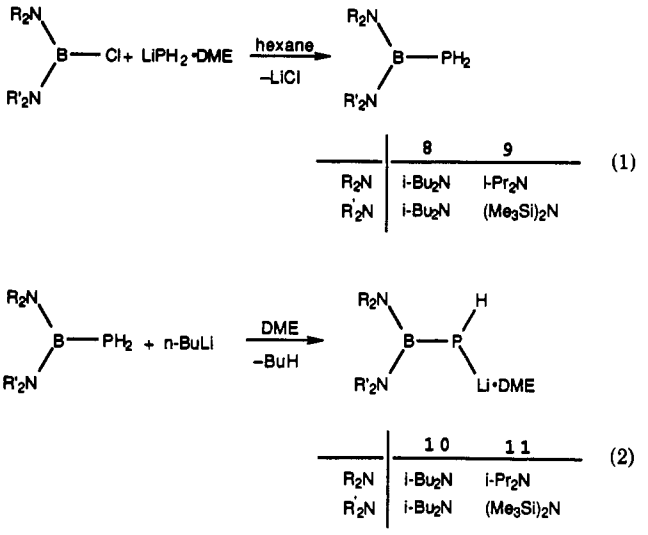

infrared frequencies in the P–H stretching region (2400–2200 cm^{-1})—**8**, 2328 and 2303 cm^{-1}; **9**, 2338 and 2324 cm^{-1}—a single resonance in the $^{31}P\{^1H\}$ NMR spectrum, and a triplet in the proton coupled ^{31}P NMR spectrum due to P–H coupling. The detailed NMR data for **8** and **9** are summarized in Table 6. The data compare favorably with those shown by $(i\text{-}Pr_2N)_2BPH_2$: ^{31}P δ −206, $^1J_{PH}$ = 208 Hz.[4] The phosphinoboranes **8** and **9** are easily deprotonated with *n*-BuLi, as shown in eq 2. The corresponding lithium phosphides **10** and **11** are obtained as a white powder and a colorless crystalline solid, respectively. Analytical and ^1H and ^{13}C NMR data indicate that **10** is obtained as a 1:1 solvate with DME, while the composition of **11** is estimated as $(i\text{-}Pr_2N)[(Me_3Si)_2N]BP(H)Li\cdot 0.84DME$. Both compounds display a single infrared band in the P–H stretching region: **10**, 2280 cm^{-1}; **11**, 2276 cm^{-1}. Their $^{31}P\{^1H\}$ NMR spectra show a single resonance that splits into a doublet in the proton-coupled spectrum. These data also compare favorably with the ^{31}P chemical shift and P-H coupling constant for $(i\text{-}Pr_2N)_2BP(H)Li\cdot DME$: ^{31}P δ −213, $^1J_{PH}$ = 170.9 Hz. The $^7Li\{^1H\}$ NMR spectra for **10** at −30 °C and **11** at 20 °C show a triplet pattern with J_{LiP} = 47 and 44 Hz, respectively. This coupling pattern is also similar to that displayed by $(i\text{-}Pr_2N)_2BP(H)Li\cdot DME$ at ~−18 °C and is consistent with dimeric formulations in benzene and toluene solutions. The dimeric structure has been confirmed in the solid state by single-crystal X-ray analysis of $[(i\text{-}Pr_2N)_2BP(H)Li\cdot DME]_2$.[4]

The reactions of $(i\text{-}Pr_2N)_2BP(H)Li\cdot DME$ with $i\text{-}Pr_2NBCl_2$, $(tmp)BCl_2$, and $(Me_3Si)_2NBCl_2$ have previously been reported to give diborylphosphanes, $(i\text{-}Pr_2N)_2BP(H)B(Cl)NR'_2$ **1a–c**.[4] In a similar fashion, the combinations of the phosphides **10** and **11** with $tmpBCl_2$ and $(Me_3Si)_2NBCl_2$ produce new diborylphosphanes **12–15** as an oil (**12**) or colorless crystalline solids, as shown in eq 3. These compounds display spectroscopic features

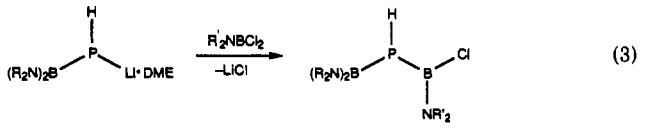

	1a	1b	1c	12	13	14	15
R_2N	$i\text{-}Pr_2N$	$i\text{-}Pr_2N$	$i\text{-}Pr_2N$	$i\text{-}Bu_2N$	$i\text{-}Bu_2N$	$i\text{-}Pr_2N[(Me_3Si)_2N]$	$i\text{-}Pr_2N[(Me_3Si)_2N]$
R'_2N	$i\text{-}Pr_2N$	tmp	$(Me_3Si)_2N$	tmp	$(Me_3Si)_2N$	tmp	$(Me_3Si)_2N$

comparable with those reported for **1**.[4] In particular, each compound displays a single infrared band assigned to ν_{PH} at 2353–

Table 5. Selected Bond Distances (Å) and Bond Angles (deg) for $(Me_3Si)_2NB\{P(H)B(N\text{-}i\text{-}Pr_2)[N(SiMe_3)_2]\}_2$ (**19**), $(Me_3Si)_2NB[P(H)B(N\text{-}i\text{-}Pr_2)_2]_2$ (**20**), and $\{[(i\text{-}Pr_2N)(Cl)B]PB(N\text{-}i\text{-}Pr_2)\}_2$ (**21**)

19		**20**	**21**
molecule 1	molecule 2		
Bond Distances			
P(1)–B(1) 1.925(8)	P(3)–B(4) 1.931(8)	P(1)–B(1) 1.924(10)	P(1)–B(1) 1.915(9)
P(1)–B(2) 1.930(8)	P(3)–B(5) 1.948(9)	P(1)–B(2) 1.958(11)	P(1)–B(2) 1.956(9)
P(2)–B(1) 1.874(8)	P(4)–B(4) 1.875(8)	P(2)–B(1) 1.917(9)	P(1)–B(1′) 1.928(8)
P(2)–B(3) 1.924(9)	P(4)–B(6) 1.935(8)	P(2)–B(3) 1.974(10)	P(1′)–B(1) 1.928(8)
B(1)–N(1) 1.456(8)	B(4)–N(6) 1.463(10)	B(1)–N(1) 1.449(10)	B(1)–N(1) 1.401(10)
B(2)–N(2) 1.473(11)	B(5)–N(7) 1.489(9)	B(2)–N(2) 1.445(12)	B(2)–N(2) 1.384(12)
B(2)–N(3) 1.414(10)	B(5)–N(8) 1.394(10)	B(2)–N(3) 1.418(12)	
B(3)–N(4) 1.485(9)	B(6)–N(9) 1.474(10)	B(3)–N(4) 1.428(13)	
B(3)–N(5) 1.403(10)	B(6)–N(10) 1.405(10)	B(3)–N(5) 1.415(12)	
			B(2)–Cl 1.763(10)
Bond Angles			
B(1)–P(1)–B(2) 126.4(4)	B(5)–P(3)–B(4) 125.2(3)	B(1)–P(1)–B(2) 123.9(4)	B(1)–P(1)–B(1′) 81.9(4)
B(2)–P(2)–B(3) 137.2(3)	B(4)–P(4)–B(6) 138.5(4)	B(2)–P(2)–B(3) 115.7(4)	B(1)–P(1)–B(2) 113.0(4)
P(1)–B(1)–P(2) 119.6(4)	P(3)–B(4)–P(4) 119.3(4)	P(1)–B(1)–P(2) 115.9(4)	B(2)–P(1)–B(1′) 108.1(4)
P(1)–B(1)–N(1) 114.6(5)	P(3)–B(4)–N(6) 115.2(5)	P(1)–B(1)–N(1) 122.7(6)	
P(2)–B(1)–N(1) 125.4(6)	P(4)–B(4)–N(6) 125.1(5)	P(2)–B(1)–N(1) 121.2(6)	
P(1)–B(2)–N(2) 116.5(5)	P(3)–B(5)–N(7) 115.8(5)	P(1)–B(2)–N(3) 124.2(7)	P(1)–B(1)–N(1) 134.9(6)
P(1)–B(2)–N(3) 119.5(6)	P(3)–B(5)–N(8) 120.2(5)	P(1)–B(2)–N(2) 114.4(7)	N(1)–B(1)–P(1′) 126.9(6)
N(2)–B(2)–N(3) 123.3(6)	N(7)–B(5)–N(8) 123.2(6)	N(2)–B(2)–N(3) 121.4(8)	P(1)–B(1)–P(1′) 98.1(4)
P(2)–B(3)–N(4) 114.5(6)	P(4)–B(6)–N(9) 115.6(5)	P(2)–B(3)–N(4) 117.4(6)	P(1)–B(2)–N(2) 121.5(7)
P(2)–B(3)–N(5) 121.6(5)	P(4)–B(6)–N(10) 121.0(6)	P(2)–B(3)–N(5) 119.8(7)	Cl–B(2)–N(2) 121.6(6)
N(4)–B(3)–N(5) 123.4(7)	N(9)–B(6)–N(10) 123.1(6)	N(4)–B(3)–N(5) 122.2(8)	P(1)–B(2)–Cl 117.0(5)

2340 cm^{-1}. The $^{31}P\{^1H\}$ NMR spectra show only one resonance as a doublet, J_{PH} = 253–226 Hz, in proton-coupled spectra. Each compound reveals two resonances of equivalent intensity in its ^{11}B NMR spectrum, and the chemical shifts fall in regions expected for the respective fragments.[3,4,18]

As mentioned in the Introduction, diborylphosphanes of the general type $(R_2N)_2BP(H)B(Cl)(NR'_2)$ are expected to undergo 1,2-dehydrohalogenation and thereby serve as precursors to P-borylated boranylidenephosphanes, **2**, or their cyclic condensation products. In our earlier study, the dehydrohalogenation of the diborylphosphane **5** (R_2N = *i*-Pr_2N, R'_2N = tmp), promoted by *t*-BuLi, produced an unexpected azacarbaphosphaboretane **7**. As outlined in Scheme 1, it is assumed that addition of *t*-BuLi to **5** results in formation of the anticipated boranylidenephosphane **6**. However, instead of dimerizing, the incipient B=P center is sufficiently reactive that it undergoes intramolecular C—H bond addition with a neighboring *i*-Pr_2NB group. Attempts to study the dehydrohalogenation of another derivative of **1** (R'_2N = *i*-Pr_2N) were thwarted because this compound is obtained only as an impure oil. The availability of **12**–**15** as pure compounds without activated isopropyl C–H groups allowed us to explore other potential dehydrohalogenation pathways for diborylphosphanes.

The reactions of **12** and **13** with *t*-BuLi give the target P-borylated diphosphadiboretanes **16** and **17**, as summarized in eq 4. Although ^{31}P NMR spectra of the reaction mixtures show

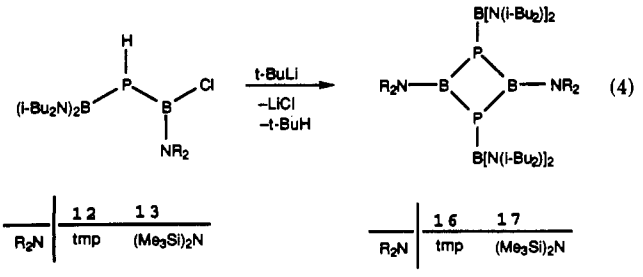

(4)

that both compounds are formed in high yield, they are isolated in only 61% and 22% yields, respectively, due to difficulties in crystallization from the crude oily reaction mixtures. It is assumed that the diphosphadiboretanes assemble by head-to-tail dimerization of respective transient boranylidene-phosphanes, $(i\text{-}Bu_2N)_2B—P{=}B(NR_2)$. Compounds **16** and **17** are yellow crystalline solids that display a parent ion in FABS-MS analyses. Infrared spectra for the compounds show no evidence for a band in the P–H stretching region, and ^{31}P NMR data show no evidence for one-bond P–H coupling. It is interesting to note that the $^{31}P\{^1H\}$ NMR resonance for **16**, δ –81.1, is significantly downfield from the resonance in the dimeric diphosphadiboretane ((tmp)BPH)$_2$, δ –127.2,[3] while the shift for **17**, δ –66.2, is very similar to the value observed for the trimer $[(Me_3Si)_2NBPH]_3$, δ –68.3.[3] The ^{11}B NMR spectra for **16** and **17** show two resonances of equal intensity with chemical shift values comparable to the resonances for the comparable dimeric and trimeric rings[3] and the $(i\text{-}Bu_2N)_2B$ fragment in **8**, **10**, and **13**.

Surprisingly, the reaction of **14** with *t*-BuLi does not proceed by either of the pathways established for $(i\text{-}Pr_2N)_2BP(H)B(Cl)$-tmp or **12** and **13**. Instead, the reaction produces a number of products, one of which is identified by NMR spectroscopy of the reaction mixture as the *mono-P-borylated* diphosphadiboretane $\{(i\text{-}Pr_2N)[(Me_3Si)_2N]BPB(tmp)P(H)B(tmp)\}$ (**18**). This compound is prepared in higher yield by combination of (tmp)BP(H)B(tmp)PLi·DME with $(i\text{-}Pr_2N)[(Me_3Si)_2N]BCl$.[19] The $^{31}P\{^1H\}$ NMR spectrum of **18** displays two resonances centered at δ –87.4 and –99.0 and both are split into a doublet with J_{pp} = 79 Hz. The lower field resonance of the pair is broader than the higher field resonance, and it is assigned to the borylated phosphorus atom. This assignment is confirmed in the proton-coupled spectrum that shows no further splitting of the downfield resonance. The two members of the higher field resonance, however, are each split into a doublet by the directly bonded hydrogen, $^1J_{PH}$ = 147 Hz.

The reaction of **15** with *t*-BuLi is also complicated and several products are produced. Among the products is an acyclic

(18) Nöth, H.; Wrackmeyer, B. In *Nuclear Magnetic Resonance Spectroscopy of Boron Compounds*; Diehl, P., Fluck, E., Kosfeld, R., Eds.; Springer-Verlag: Berlin, 1978.

(19) Dou, D. Ph.D. Thesis, University of New Mexico, 1992.

(20) Bartlett, R. A.; Dias, H. v. R.; Power, P. P. *Inorg. Chem.* **1988**, *27*, 3919.

(21) Karsch, H. H.; Hanika, G.; Huber, B.; Mundle, K.; Krönig, S.; Krüger, C.; Müller, G. *J. Chem. Soc., Chem. Commun.* **1989**, 373.

diphosphatriboretane $[(Me_3Si)_2N]B\{P(H)B(i\text{-}Pr_2N)[(Me_3Si)_2N]\}_2$ (**19**) obtained in 32% yield, as represented in eq 5. This compound

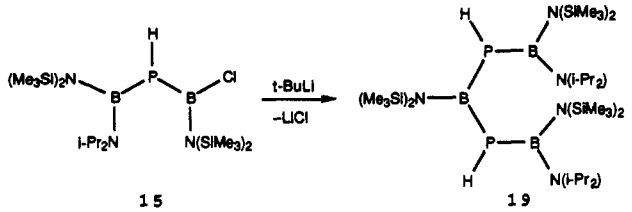

15 19 (5)

is produced more directly in higher yield (59%) from the 1:2 reaction of $(Me_3Si)_2NBCl_2$ with **11**. Compound **19** is stable at 23 °C, and it shows no sign of phosphane elimination accompanied by formation of a diphosphadiboretane derivative. The $^{31}P\{^1H\}$ NMR spectrum reveals a single peak, δ −70.5, which is split into a doublet by P–H coupling, J_{PH} = 288 Hz. The ^{11}B NMR spectrum shows two resonances at δ 65.0 and 37.8 in a 1:2 area ratio. It is also important to note that this reaction proceeds as shown despite the availability of an *i*-Pr_2N group on the bis(amido)-substituted boron atom. There is no evidence for attack of an isopropyl C—H bond on a potentially available incipient B=P double bond (Scheme 1). To further explore this point, the reaction of one of the previously described diborylphosphanes **1**, $(i\text{-}Pr_2N)_2BP(H)B(Cl)[N(SiMe_3)_2]$,[3] with *t*-BuLi was examined. This reaction is particularly sluggish and the diphosphatriboretane **20** was obtained in low yield (11%), as shown in eq 6. No evidence

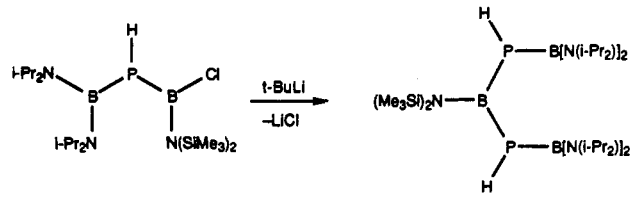

20 (6)

for the formation of an azacarbaphosphaboretane analogue of **7** was seen. Compound **20** is characterized by the appearance of a P–H stretching frequency at 2311 cm^{-1} in the infrared spectrum and by appropriate ^{31}P and ^{11}B NMR spectra. The $^{31}P\{^1H\}$ NMR spectrum displays a singlet at δ −101.4 that splits into a doublet in the proton-coupled spectrum, $^1J_{PH}$ = 276 Hz. The ^{11}B NMR spectrum shows two resonances at δ 67.5 and 37.7 in a 1:2 area ratio that are assigned to the $(Me_3Si)_2NB$ and $[(i\text{-}Pr_2N)_2B]$ fragments.

Single crystals of **19** and **20** were obtained, and the molecular structures were determined by X-ray diffraction analyses. Views of the molecules are presented in Figures 1 and 2, and selected bond distances and angles are summarized in Table 5. The structures confirm that these compounds exist as B–P(H)–B–P(H)–B acyclic chains. Each phosphorus atom is pyramidal and all boron and nitrogen atoms are trigonal planar. The two P–H bond vectors are oriented in an *anti* configuration. All of the P–B bond distances fall in a range expected for single bonds, and it is interesting that three of the four B–P bond distances in **19**, (molecule 1, P(1)–B(2), P(1)–B(1), and P(2)–B(3); molecule 2, P(3)–B(5), P(3)–B(4), and P(4)–B(6)) are identical (average over both molecules, 1.932(8) Å (range: 1.925(8)–1.948(9)Å). The fourth distance is slightly shorter (molecule 1, P(2)–B(1) = 1.874(8) Å; molecule 2, P(4)–B(4) = 1.875(8) Å).

The trend in B–P bond distances in **20** is somewhat more regular, although reliable comparisons are weakened by the large esd's. The two internal distances P(1)–B(1) and P(2)–B(1) are identical (average 1.920(10) Å) and shorter than the two external distances P(1)–B(2) and P(2)–B(3) (average 1.966(11) Å). The variations in **20** are consistent with stronger B–P π orbital overlap in the monoaminoborane fragment than in the diaminoborane fragments. A similar trend was found in the structure of (tmp)B(Cl)P(H)B(N-*i*-Pr_2)$_2$ where the B–P bond distance in the (tmp)B(Cl)–P fragment is 1.925(5) Å, and the $(i\text{-}Pr_2N)_2B$–P bond distance is 1.979(5) Å. These observations suggest that the P(1)–B(1) and P(3)–B(4) bond distances in **19** (molecules 1 and 2) should be shorter than observed, so there may be additional features affecting these distances. The P–B distances may be compared with the average distances found in $(Ph_2P)_2B(Mes)$, 1.899 Å, $Ph_2NB[P(SiMe_3)_2]_2$, 1.896 Å, and the cyclic trimer $[(Me_3Si)_2NBPH]_3$, 1.928 Å. The average B–N bond distances in **19** (molecules 1 and 2) fall into two logical groups involving B–N(*i*-Pr_2), 1.408 Å, and B–N$(SiMe_3)_2$, 1.473 Å. As expected, the average B–N(*i*-Pr_2) distance is shorter due to more efficient B–N π overlap. Unfortunately, the esd's of the B–N distances in **20** are large, and the average B–N bond distances for the B–N(*i*-Pr_2)$_2$ and B–N$(SiMe_3)_2$ groups must be considered equivalent.

The details of the mechanism for formation of **19** and **20** have not yet been elucidated; however, it can be concluded that the (tmp)B fragment in **5** is apparently more prone to C–H bond attack than is the $(Me_3Si)_2NB$ fragment, and this may have an origin in the differing degrees of B=N π bonding in these fragments. Further NMR studies of the evolution of these reactions will be required to confirm this point.

In related chemistry, we have succeeded in preparing several other monoborylated diphosphadiboretanes (**22**) by reaction of $R_2NBP(H)B(NR_2)PLi\cdot DME$ with R'_2NBCl_2, as described in eq 7.[22] Base-promoted dehydrohalogenation of these compounds

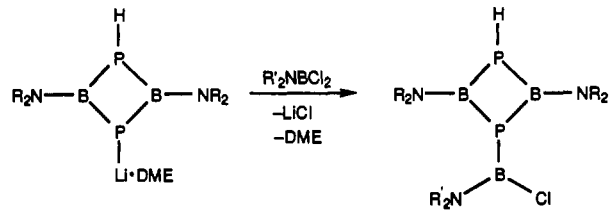

22 (7)

provides a high-yield route to several $(R_2NB)_2(R'_2NB)P_2$ bicyclic trigonal bipyramidal cage compounds. It proved impossible to isolate one of these monoborylated diphosphadiboretanes, R_2N = *i*-Pr_2N, R'_2N = *i*-Pr_2N, since the compound is prone to dehydrohalogenate spontaneously even in the absence of base. We have continued to examine this particular 1:1 reaction and report here the unexpected formation of the diborylated diphosphadiboretane **21** in low yield (5–10%). The $^{31}P\{^1H\}$ NMR

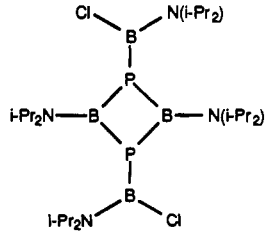

21

spectrum of **21** displays one resonance at δ −110, and its $^{11}B\{^1H\}$ NMR spectrum displays two resonances in equal intensity at δ 48.1 and 39.9.

(22) Dou, D.; Wood, G. L.; Duesler, E. N.; Paine, R. T.; Nöth, H. *Inorg. Chem.* **1992**, *31*, 3756.

Table 6. NMR Data for Boron–Phosphorus Compounds

compound	$\delta(^{11}B\{^1H\})$	$\delta(^{31}P\{^1H\})$	$\delta(^1H)$	$\delta(^{13}C\{^1H\})$	δ(Li)
$(i\text{-}Bu_2N)_2BPH_2$ (**8**)	38.1	−228.2	2.7 (C_1H)	57.6 (C_2)	
			1.8 (C_2H)	27.5 (C_1)	
			0.8 (C_3H)	20.5 (C_3)	
			1.9 (PH)		
$(i\text{-}Pr_2N)[(Me_3Si)_2N]BPH_2$ (**9**)	40.3	−184.9	4.6 (C_2H)	47.3 (C_2)	
			3.1 (C_1H)	44.6 (C_1)	
			1.2 (C_3H)	24.0 (C_3)	
			0.9 (C_4H)	21.4 (C_4)	
			0.25 ($SiMe_3$)	3.5 ($SiMe_3$)	
			2.3 (PH)		
$(i\text{-}Bu_2N)_2BP(H)Li\cdot DME$ (**10**)	47.4	−247.8	3.3 (DME)	70.3 (DME)	1.62
			3.2 (DME)	59.4 (DME)	
			3.0 (C_1H)	57.4 (C_2)	
			2.1 (C_2H)	27.1 (C_1)	
			1.0 (C_3H)	21.2 (C_3)	
$(i\text{-}Pr_2N)[(Me_3Si)_2N]BP(H)Li\cdot 0.84DME$ (**11**)	45.0	−183.2	4.9 (C2H)	70.2 (DME)	1.64
			3.5 (C1H)	57.2 (DME)	
			3.2 (DME)	46.1 (C_2)	
			3.1 (DME)	45.7 (C_1)	
			1.6 (C_3H)	24.1 (C_3)	
			1.2 (C_4H)	22.6 (C_4)	
			0.49 ($SiMe_3$)	4.3 ($SiMe_3$)	
(tmp)B(Cl)P(H)B(N-i-Bu_2)$_2$ (**12**)	46.4 (tmpB)	−156.8	3.0 (C_1H)	57.4 (C_2)	
	37.7 [(i-Bu_2N)$_2$B]		1.9 (C_2H)	56.5 (tmp)	
			1.6 (tmp)	36.0 (tmp)	
			1.5 (tmp)	31.9 (tmp)	
			0.9 (C_3H)	26.6 (C_1)	
			2.7 (PH)	20.8 (C_3)	
$[(Me_3Si)_2N](Cl)BP(H)B(N\text{-}i\text{-}Bu_2)_2$ (**13**)	53.7 [$(Me_3Si)_2NB$]	−150.8	3.0 (C_1H)	57.4 (C_2)	
	37.2 [(i-Bu_2N)$_2$B]		1.9 (C_2H)	26.6 (C_1)	
			0.9 (C_3H)	20.7 (C_3)	
			0.4 ($SiMe_3$)	4.3 ($SiMe_3$)	
			2.5 (PH)		
tmp(Cl)BP(H)B(N-i-Pr_2)[$(Me_3Si)_2N$] (**14**)	45.0 (tmpB)	−117.4	4.7 (C_1H)	56.7 (tmp)	
	39.1 [(i-Pr_2N)$(Me_3Si)_2NB$]		4.4 (C_2H)	51.6 (C_2)	
			1.6 (tmp)	47.2 (C_1)	
			1.5 (tmp)	36.1 (tmp)	
			1.4 (C_4H)	32.4 (tmp)	
			1.2 (C_3H)	24.6 ($C_{3,4}$)	
			0.36 ($SiMe_3$)	14.8 (tmp)	
			2.8 (PH)	4.0 ($SiMe_3$)	
$[(Me_3Si)_2N](Cl)BP(H)BP(N\text{-}i\text{-}Pr_2)[(Me_3Si)_2N]$ (**15**)	51.7 [$(Me_3Si)_2NB(Cl)$]		4.6 (C_1H)	50.6 (C_2)	
	37.9 [(i-Pr_2N)$(Me_3Si)_2NB$]		4.0 (C_2H)	47.6 (C_1)	
			1.2 (C_4H)	24.7 (C_4)	
			1.1 (C_3H)	23.9 (C_3)	
		−107.6	0.38 (Me_3Si)	4.4 ($SiMe_3$)	
			0.34 (Me_3Si)	3.9 ($SiMe_3$)	
			2.8 (PH)		
[(i-Bu_2N)$_2$BPB(tmp)]$_2$ (**16**)	58.4 (tmpB)	−81.1	3.3 (C_1H)	59.0 (C_2)	
	36.0 [(i-Bu_2N)$_2$B]		2.0 (C_2H)	55.7 (tmp)	
			1.8 (tmp)	38.2 (tmp)	
			1.7 (tmp)	35.0 (tmp)	
			1.0 (C_3H)	28.0 (C_1)	
				21.9 (C_3)	
				16.3 (tmp)	
{(i-Bu_2N)$_2$BPB[$N(SiMe_3)_2$]}$_2$ (**17**)	70.4 [$(Me_3Si)_2NB$]	−66.2	3.1 (C_1H)	58.4 (C_2)	
	34.2 [(i-Bu_2N)$_2$B]		1.9 (C_2H)	27.6 (C_1)	
			1.0 (C_3H)	21.7 (C_3)	
			0.56 (Me_3Si)	5.3 (Me_3Si)	
{(i-Pr_2N)[$(Me_3Si)_2N$]BPB(tmp)P(H)B(tmp)} (**18**)	50.4 (tmp B)		4.8 (C_2H)	57.0 (tmp)	
	38.2 {[$(Me_3Si)_2N$](i-Pr_2N)B]		4.8 (C_2H)	57.0 (tmp)	
	38.2 {[$(Me_3Si)_2N$](i-Pr_2N)B]		4.6 (C_1H)	51.4 (C_1)	
		−87.4	1.6 (tmp)	46.6 (C_2)	
		−99.0	1.5 (tmp)	41.6 (tmp)	
			1.3 (C_3H)	33.5 (tmp)	
			1.2 (C_4H)	25.8 (C_4)	
			0.18 (Me_3Si)	25.7 (C_3)	
			5.4 (PH)	16.6 (tmp)	
				4.2 (Me_3Si)	
$[(Me_3Si)_2N]B\{P(H)B(i\text{-}Pr_2N)[(Me_3Si)_2N]\}_2$ (**19**)	65.0 [$(Me_3Si)_2NB$]		4.6 (C_1H)	52.9 (C_2)	
	37.8 {[$(Me_3Si)_2N$](i-Pr_2N)B}		4.2 (C_2H)	47.1 (C_1)	
			1.4 (C_4H)	25.4 (C_4)	
			1.2 (C_3H)	25.0 (C_3)	
		−70.5	0.45 (Me_3Si)	4.7 (Me_3Si)	
			0.36 (Me_3Si)	4.0 (Me_3Si)	
			2.8 (PH)		

Table 6 (Continued)

compound	$\delta(^{11}B\{^1H\})$	$\delta(^{31}P\{^1H\})$	$\delta(^1H)$	$\delta(^{13}C\{^1H\})$	δ(Li)
$[(Me_3Si)_2N]B[P(H)B(i\text{-}Pr_2N)_2]_2$ (**20**)	67.5 [$(Me_3Si)_2NB$] 37.7 [$(i\text{-}Pr_2N)_2B$]	−101.4	3.9 (C_1H) 1.3 (C_2H) 0.5 (Me_3Si) 2.8 (PH)	49.2 (C_1) 25.2 (C_2) 5.1 (Me_3Si)	
$\{[(i\text{-}Pr_2N)(Cl)B]PB(N\text{-}i\text{-}Pr_2)\}_2$ (**21**)	48.1 [$(i\text{-}Pr_2N)BCl$] 39.9 [$(i\text{-}Pr_2N)_2B$]	−110.0			
$(CO)_5Cr$ (**21**)	43.1 [$(i\text{-}Pr_2N)BCl$] 37.3 [$(i\text{-}Pr_2N)_2B$]				
$(CO)_3Fe$ (**21**)	43.2 [$(i\text{-}Pr_2N)BCl$] 37.3 [$(i\text{-}Pr_2N)_2B$]	−98.2			

[a] 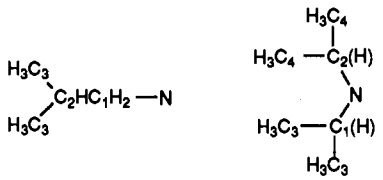

[b] Coupling constants (Hz): **8**, $^1J_{PH}$ = 201.8, $^4J_{CP}$ = 4.3, $^3J_{HH}$ = 7.4, $^3J_{HH}$ = 6.8, $^3J_{HH}$ = 6.6; **9**, $^1J_{PH}$ = 210.9, $^4J_{CP}$ = 5.1, $^3J_{HH}$ = 7.1, $^3J_{HH}$ = 6.7, $^3J_{HH}$ = 7.1, $^3J_{HH}$ = 6.8; **10**, $^1J_{PH}$ = 177.2, $^3J_{HH}$ = 7.3, $^3J_{HH}$ = 6.7, $^3J_{HH}$ = 6.6, $^1J_{LiP}$ = 47; **11**, $^1J_{PH}$ = 163.8, $^3J_{HH}$ = 6.9, $^3J_{HH}$ = 6.8, $^3J_{HH}$ = 6.9, $^3J_{HH}$ = 6.8, $^1J_{LiP}$ = 44; **12**, $^1J_{PH}$ = 226.4, $^4J_{CP}$ = 5.0, $^3J_{HH}$ = 7.2, $^3J_{HH}$ = 6.7, $^3J_{HH}$ = 6.6; **13**, $^1J_{PH}$ = 226.4, $^4J_{CP}$ = 4.9, $^4J_{CP}$ = 2.2, $^3J_{HH}$ = 7.3, $^3J_{HH}$ = 6.7, $^3J_{HH}$ = 6.6; **14**, $^1J_{PH}$ = 238.2, $^3J_{CP}$ = 15.1, $^4J_{CP}$ = 5.7, $^4J_{CP}$ = 4.7, $^3J_{HH}$ = 7.0, $^3J_{HH}$ = 7.0; **15**, $^1J_{PH}$ = 253.1, $^3J_{CP}$ = 11.2, $^4J_{CP}$ = 0.9, $^4J_{CP}$ = 2.5, $^3J_{HH}$ = 7.0, $^3J_{HH}$ = 7.1; **16**, $^3J_{CP}$ = 5.1, $^3J_{HH}$ = 6.5, $^3J_{HH}$ = 6.6, $^3J_{HH}$ = 6.6; **17**, $^3J_{HH}$ = 6.8, $^3J_{HH}$ = 6.6, $^3J_{HH}$ = 6.6; **18**, J_{PP} = 79, $^1J_{PH}$ = 147.7, $^3J_{HH}$ = 6.9, $^3J_{HH}$ = 7.1, $^4J_{PH}$ = 2.0, $^3J_{HH}$ = 7.0, $^3J_{HH}$ = 7.1; **19**, $^1J_{PH}$ = 288, $^3J_{CP}$ = 7.5, $^3J_{HH}$ = 7.2, $^3J_{HH}$ = 7.0, $^3J_{HH}$ = 7.2, $^3J_{HH}$ = 7.0; **20**, $^1J_{PH}$ = 276, $^3J_{HH}$ = 6.9, $^3J_{HH}$ = 6.9.

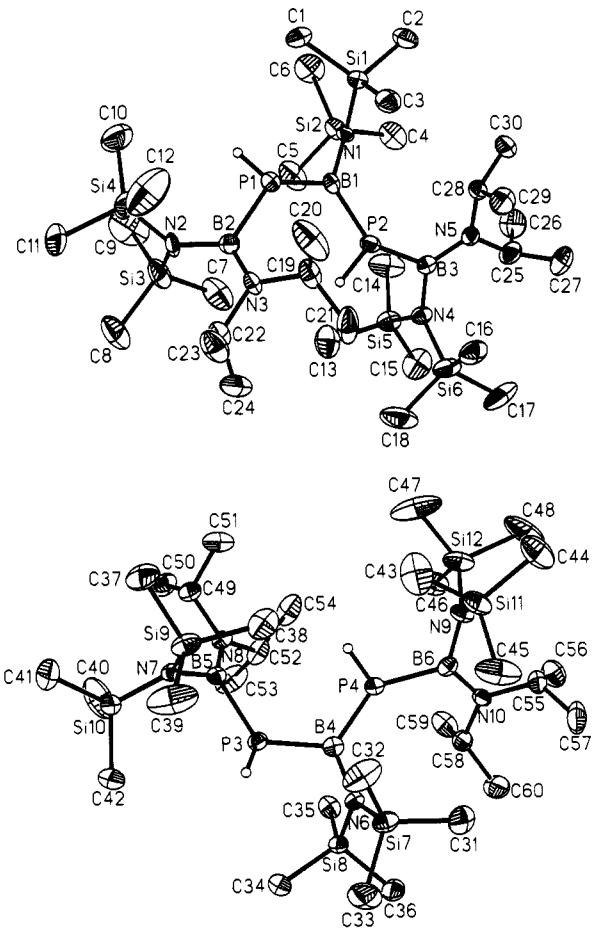

Figure 1. Molecular structure and atom labeling scheme for $(Me_3Si)_2NB\{P(H)B(N\text{-}i\text{-}Pr_2)[N(SiMe_3)_2]\}_2$ (**19**): (a, top) molecule 1; (b, bottom) molecule 2. Hydrogen atoms on carbon atoms are omitted for clarity.

We have previously pointed out[3] that double deprotonation of the diphosphadiboretane $(i\text{-}Pr_2NBPH)_2$ with 2 equiv of base is not accomplished in significant amounts with *n*-BuLi, *t*-BuLi, or K. However, formation of a small amount of the dianion in these solutions cannot be ruled out. Indeed, reaction of the dianion species with $i\text{-}Pr_2NBCl_2$ could provide a route to **21**. Compound **21** may also form sequentially by deprotonation of **22** with a small amount of $LiPH_2$ used to form the precursor lithium salt of the diphosphadiboretane followed by addition of $i\text{-}Pr_2NBCl_2$. Alternatively, **22** might redistribute, thereby forming **21** and diphosphadiboretane $(i\text{-}Pr_2NBPH)_2$. Compound **22** may also be deprotonated by $i\text{-}Pr_2NBP(H)B(N\text{-}i\text{-}Pr_2)PLi\cdot DME$, and the resulting anion may react with $i\text{-}Pr_2NBCl_2$, giving **21** and $(i\text{-}Pr_2NBPH)_2$. The last two processes are plausible since the formation of $(i\text{-}Pr_2NBPH)_2$ is indicated in ^{31}P NMR spectra of the reaction mixture, although the relative amounts of **21** and $(i\text{-}Pr_2NBPH)_2$ are ~5:1.

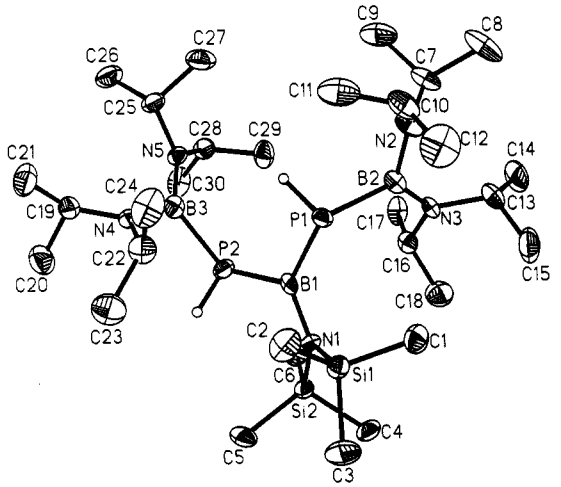

Figure 2. Molecular structure and atom labeling scheme for $(Me_3Si)_2NB[P(H)B(N\text{-}i\text{-}Pr_2)_2]_2$ (**20**). Hydrogen atoms on carbon atoms are omitted for clarity.

We also found that **21** is unexpectedly formed from the 1:1 reaction of $(MeN)_3(MeB)_2BP(H)Li\cdot DME$ with $i\text{-}Pr_2NBCl_2$, as described in eq 8. The 1-chloropentamethylborazine is obtained in about 60% yield, and **21** is isolated in about 30% yield. The driving force for this reaction appears to be the formation of the particularly stable 1-chloropentamethylborazine.

The molecular structure of **21** was determined by single-crystal X-ray analysis, and a view is shown in Figure 3. The planar, four-membered P_2B_2 ring is a rhombus with planar boron atoms and pyramidal phosphorus atoms. The *endo* ring P–B bond distances of 1.928(8) and 1.915(9) Å compare favorably with the average P–B distance in $(i\text{-}Pr_2NBPH)_2$, 1.931(3) Å. The *exo*

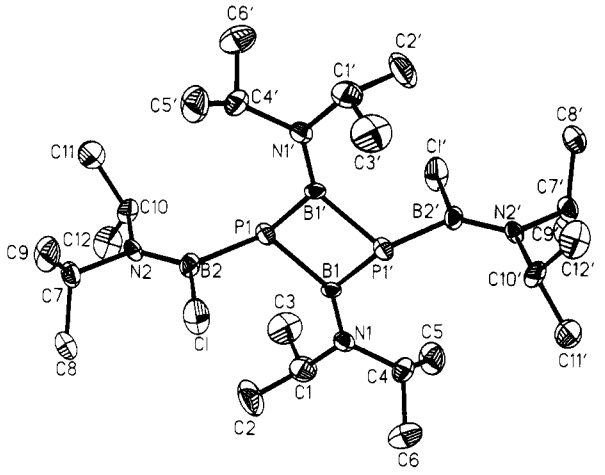

Figure 3. Molecular structure and atom labeling scheme for {[(*i*-Pr_3N)(Cl)B]PB(N-*i*-Pr_2)}$_2$ (**21**). Hydrogen atoms on carbon atoms are omitted for clarity.

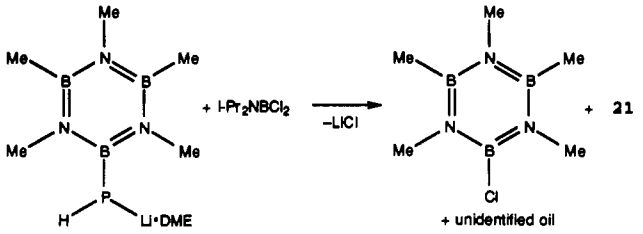

(8)

B–P distance in **21**, 1.956(9) Å, is relatively long, indicating weaker B–P overlap. The B(1)–N(1) and B(2)–N(2) distances are 1.401(10) and 1.384(12) Å, respectively, and for comparison, the B–N distance in (*i*-$Pr_2NBPH)_2$ is 1.377(3) Å. All are relatively short and indicative of B=N π bonding that clearly competes effectively against potential *endo* and *exo* B–P π overlap.

Some coordination chemistry of **21** has also been examined. In particular, the 1:1 combination of **21** with $Cr(CO)_5{\cdot}NMe_3$ gives yellow crystalline $(CO)_5Cr$(**21**). Its composition is confirmed by elemental analysis and the appearance of a parent ion envelope in the high resolution FAB-MS spectrum. An IR spectrum shows three bands in the terminal carbonyl stretching region at 2054, 1956, and 1929 cm^{-1}. The band pattern resembles those displayed by $Cr(CO)_5$ complexes of several diphosphadiboretanes.[3] The $^{11}B\{^1H\}$ NMR spectrum shows two resonances at δ 43.1 and 37.3 assigned to the *endo* and *exo* *i*-Pr_2NB fragments, respectively.

In past studies, we found that reactions of diphosphadiboretanes with $Fe_2(CO)_9$ typically give monometallic adducts in which a $Fe(CO)_4$ unit is bonded to one of the two phosphorus donor sites. In **21**, however, reaction with $Fe_2(CO)_9$ gives a gold-brown solid with a composition $(CO)_3Fe$(**21**) fixed by elemental analysis and the appearance of a parent ion envelope in the high resolution FAB-MS spectrum. Given this composition and the structure of **21**, the ligand should bind in a bidentate fashion with the two phosphorus atoms occupying *cis* positions on a trigonal bipyramidal $(\widehat{LL})FeCO_3$ fragment [$(\widehat{LL})$ = bidentate ligand]. The infrared spectrum of this complex (C_s symmetry) would be predicted to display three terminal CO stretching frequencies (2a′ + a″). The infrared spectrum obtained in this case, however, displays four terminal carbonyl bands at 2035, 1958, 1931, and 1919 cm^{-1}. One of these bands may arise from an impurity species. The $^{11}B\{^1H\}$ NMR spectrum reveals two resonances at δ 43.2 and 37.3 assigned to the *endo* and *exo* *i*-Pr_2NB groups, respectively. The $^{31}P\{^1H\}$ NMR spectrum displays one resonance at δ 98.2. Unfortunately, all attempts to obtain single crystals of this interesting complex have so far failed.

Acknowledgment. Acknowledgment is made to the National Science Foundation (Grant CHE-8503550) (R.T.P.) and the Fonds der Chemischen Industrie (H.N.) for partial support of this work. Support from the Department of Energy URIP (Grant DE-FG05-86ER-75294) assisted purchase of the JEOL GSX-400 NMR spectrometer, and funds from the NSF (Grant CHE-8807358) aided purchase of the Bruker WP-250 NMR spectrometer. Selected mass spectral determinations were made at the Midwest Center for Mass Spectrometry with partial support by the NSF Biology Division (Grant DIR 9017262).

Supplementary Material Available: Tables containing additional details on the X-ray data collection and refinement, hydrogen atom coordinates, anisotropic thermal parameters, and a complete listing of bond distances and angles (46 pages). Ordering information is given on any current masthead page.